



**University of  
Zurich**<sup>UZH</sup>

**Zurich Open Repository and  
Archive**

University of Zurich  
University Library  
Strickhofstrasse 39  
CH-8057 Zurich  
[www.zora.uzh.ch](http://www.zora.uzh.ch)

---

Year: 2012

---

## **Monitoring brain repair in stroke using advanced magnetic resonance imaging**

Sztriha, Laszlo K ; O’Gorman, Ruth L ; Modo, Michel ; Barker, Gareth J ; Williams, Steven C R ;  
Kalra, Lalit

DOI: <https://doi.org/10.1161/STROKEAHA.111.649244>

Posted at the Zurich Open Repository and Archive, University of Zurich

ZORA URL: <https://doi.org/10.5167/uzh-68068>

Journal Article

Accepted Version

Originally published at:

Sztriha, Laszlo K; O’Gorman, Ruth L; Modo, Michel; Barker, Gareth J; Williams, Steven C R; Kalra, Lalit (2012). Monitoring brain repair in stroke using advanced magnetic resonance imaging. *Stroke*, 43(11):3124-3131.

DOI: <https://doi.org/10.1161/STROKEAHA.111.649244>

## **Monitoring brain repair in stroke using advanced magnetic resonance imaging**

Laszlo K Sztriha PhD, Ruth L O’Gorman PhD, Michel Modo PhD, Gareth J Barker PhD, Steven CR Williams PhD, and Lalit Kalra PhD

Departments of Clinical Neuroscience (L.K.S., L.K.) and Neuroimaging (G.B., S.W.), Institute of Psychiatry, King's College London, London, UK;  
MR Center (R.O.G.), University Children’s Hospital, Zurich, Switzerland; and  
Department of Radiology & McGowan Centre for Regenerative Medicine (M.M.), University of Pittsburgh Medical Centre, Pittsburgh, USA

**Correspondence:** Laszlo Sztriha, King’s College London, Denmark Hill, SE5 8AF, London, UK, e-mail: [laszlo.sztriha@kcl.ac.uk](mailto:laszlo.sztriha@kcl.ac.uk); Tel:+442032997784, Fax:+442078485186

**Cover Title:** MRI of brain repair after stroke

**Word count:** 6809

**Table 1.** MR options for imaging post-stroke recovery

**This manuscript contains 3 figures**

**Key words:** Angiogenesis, Brain Imaging, Brain Recovery, MRI, MR Spectroscopy, Neurogenesis, Stroke Recovery

**Subject Codes:** [30] CT and MRI, [47] Brain Circulation and Metabolism, [61] Other imaging, [65] Rehabilitation, Stroke

## Introduction

Thrombolysis and endovascular interventions have revolutionised stroke treatment, but many patients are excluded from such therapies, and residual disability is common.<sup>1</sup> Emerging approaches to enhance post-stroke brain repair may have no time constraints and are applicable to most stroke patients. Novel interventions to enhance brain repair include electromagnetic or robotic techniques, brain-computer interface, and restorative cell-based and pharmacological therapies.<sup>2-4</sup> A major impediment to translation to patient care, however, is the lack of robust *in vivo* techniques to monitor the effects of such interventions in humans.<sup>3</sup>

Non-invasive imaging of the human brain for multi-parametric *in vivo* monitoring of post-stroke recovery presents challenges. The clinical application of certain techniques such as positron emission tomography (PET) is frequently restricted by radiation exposure, limited resolution, high cost, or difficult access.<sup>5-7</sup> Magnetic resonance (MR) imaging (MRI) on the other hand is accessible, non-invasive, safe and versatile with high resolution, making this an ideal modality for multi-parametric *in vivo* monitoring of stroke recovery. This review will concentrate on MRI markers of stroke recovery in experimental models and, where available, in humans (Table 1).

## Biological substrates of neural repair

### *Angiogenesis*

The peri-infarct cortex is a unique neurovascular niche, within which angiogenesis is closely and causally linked to neurogenesis through vascular growth factors and chemokines.<sup>2</sup>

Together with parenchymal astrocytes, angiogenic vessels facilitate synaptogenesis and

axonal sprouting.<sup>2</sup> Angiogenesis stimulated by cell-based or pharmacological interventions correlates with improved behavioural outcome.<sup>2</sup> In rodents, capillary sprouting at the ischemic boundary leads to new vessel development between 2 and 28 days.<sup>8</sup> Angiogenesis has been observed in the ischemic penumbra of humans 3 to 4 days after stroke, and higher cerebral blood vessel density has been associated with improved survival.<sup>9</sup> Angiogenic vessels are permeable during the early stages of development and become less leaky as they mature, potentially allowing new vessels to be distinguished by imaging techniques.<sup>10</sup>

### ***Neurogenesis***

In experimental stroke, focal ischemia increases neurogenesis in distinct parts of the ipsilateral subependymal zone (SEZ), and neuroblasts migrate from the SEZ to the ischemic boundary regions, where they exhibit phenotypes of mature neurons (Figure1).<sup>11-13</sup> It has been shown in rat models that migration of immature cells from the SEZ occurs over the first 2 weeks, but can be sustained for several months.<sup>14</sup> Neurogenesis after stroke has been associated with functional recovery in mice.<sup>15</sup> In humans, post-mortem studies have demonstrated active proliferation of astrocytes, neuroblasts, migrating neuroblasts and immature neurons in the ipsilateral SEZ at 10 days after stroke.<sup>16-18</sup> Cells expressing markers of new-born neurons have been detected in the ischemic penumbra of humans, where they cluster around blood vessels.<sup>16, 19</sup>

### ***Axonal remodeling***

It has been shown in rats that neurons in the surviving peri-infarct cortex are induced to express a growth-associated genetic profile that enhances axonal sprouting and mediates the formation of new connections.<sup>20</sup> In experimental stroke, axonal sprouting occurs in a growth-permissive zone outside the glial scar within the peri-infarct cortex, and also up to several

millimetres away from the infarct.<sup>21</sup> Significantly increased axonal connections, originating from the peri-infarct motor cortex, have been demonstrated during recovery in rodent and primate models, correlating well with behavioural outcome.<sup>22, 23</sup>

## **Imaging of Biological Substrates**

### ***Angiogenesis***

Although direct depiction of microvessels with MR angiography is not feasible due to its relatively low spatial resolution, there are many MRI parameters that can be used to monitor angiogenesis and vascular remodeling after stroke indirectly (Table 1).<sup>24, 25</sup>

Hemodynamic parameters affected by angiogenesis, such as cerebral blood volume (CBV) and cerebral blood flow (CBF), can be measured with perfusion techniques such as dynamic susceptibility contrast-enhanced (DSC-) MRI or arterial spin labelling (ASL).<sup>25</sup> DSC-MRI calculates cerebral hemodynamic parameters from the time course of signal changes induced by the first passage of an intravenously injected paramagnetic contrast agent.<sup>26</sup> DSC-MRI has demonstrated significantly increased CBV in the recovering ipsilesional cortex of rodent stroke models, which correlated well with increased vascular density on histology.<sup>27, 28</sup> The ASL method applies radiofrequency pulses to alter the magnetisation of water protons in arterial blood, thereby generating an endogenous intravascular tracer.<sup>29</sup> Using ASL, a significantly enhanced CBF has been demonstrated in the perilesional cortex in rat models, that correlated with vascular density.<sup>28, 30</sup>

The low specificity of DSC-MRI or ASL for angiogenesis may be overcome by steady state susceptibility contrast-enhanced (SSCE)-MRI, which allows estimation of blood volume,

vessel size, and microvessel density.<sup>25</sup> The ratio of changes in gradient-echo to spin-echo relaxation rate ( $\Delta R_2^*/\Delta R_2$ ) induced by a high-molecular weight intravascular contrast agent provides an estimate of average vessel size after accounting for echo time, contrast concentration, and the main magnetic field.<sup>31</sup> The ratio  $Q \equiv \Delta R_2/(\Delta R_2^*)^{2/3}$  characterises microvascular density (MVD).<sup>32</sup> In a rat model of transient cerebral ischemia, SSCE-MRI showed decrease in vascular density and increase in vessel size due to strengthened collateral circulation in the re-perfused cortex at days 1 and 3, confirmed on histology, followed by an increase in vascular density likely attributable to angiogenesis at days 14 and 21.<sup>33</sup>

Increased permeability of the blood-brain-barrier around newly formed vessels can be assessed in humans and animal models with dynamic contrast-enhanced (DCE-) MRI, which measures the time-course of contrast-induced changes in the  $T_1$  relaxation time constant due to contrast agent extravasation into tissue.<sup>34</sup> The blood-brain-barrier transfer constant,  $K_i$ , can be estimated by locally assessing the dynamics of the signal intensity of a time-series of  $T_1$ -weighted MR images with tracer kinetic models.<sup>35</sup> In a rat stroke model,  $K_i$  in the ischemic boundary correlated with histologically confirmed angiogenesis after cell-based treatment.<sup>27</sup> The increase of  $K_i$ , peaking at 2-3 weeks, co-localized with elevated CBF and CBV at 6 weeks after cell therapy. In another study,  $K_i$  elevation was detected 1-3 weeks after stroke in sildenafil treated animals compared with 1-6 weeks in controls, suggesting that therapy accelerates angiogenesis and this is measurable with imaging.<sup>36</sup>

Newly developed vasculature rich in venous blood can be detected with blood oxygenation level-dependent (BOLD) MRI.<sup>36</sup> This exploits the local magnetic field disturbances induced by the relatively high magnetic susceptibility of deoxygenated haemoglobin, which provides  $T_2$  contrast on spin echo images and a larger  $T_2^*$  contrast on gradient echo images.<sup>37</sup>

Susceptibility weighted imaging (SWI), a variant of  $T_2^*$  weighted MRI that includes phase information, can further enhance the contrast of the areas with increased magnetic susceptibility.<sup>24, 38</sup> In a rat model of stroke, perilesional angiogenesis was successfully identified on  $T_2^*$  and SWI maps.<sup>36</sup> These techniques also detected an accelerated angiogenic profile with sildenafil, and regions exhibiting  $T_2^*$  shortening spatially matched with those with elevated  $K_i$ .<sup>36</sup>  $T_2^*$  shortening in the ischemic hemisphere spatiotemporally corresponded with increased CBF on ASL in rats.<sup>30</sup>

MRI can be used to measure haemodynamic parameters, microvascular density, blood-brain barrier permeability, and deoxygenated haemoglobin, all of which are potential markers of angiogenesis and vascular remodeling. However, MRI is not without limitations and MRI techniques differ in their availability and suitability for clinical use. MRI measurement algorithms are also based on relatively basic biophysical and mathematical models which may be inaccurate under complex or altered conditions seen with stroke.<sup>25</sup>

DSC-MRI is arguably the most widely available perfusion MRI technique in the clinical setting, but DSC-MRI methods are not fully quantitative, and thus provide information with regard to the *relative* CBF and CBV.<sup>39</sup> BOLD methods are also widely available and easily implemented but are again able to provide only a *qualitative* assessment of deoxyhaemoglobin concentration or  $T_2^*$ . ASL methods are arguably more quantitative and in recent years have become increasingly available, although most ASL methods do not provide a measure of CBV.<sup>39</sup> Both DSC-MRI and ASL are sensitive to errors arising from an increase in arterial transit time to the peri-infarct tissue, and DSC-MRI perfusion values can also be confounded by dispersion of the tracer input function or  $T_1$  changes from blood brain barrier disruption.<sup>39</sup> In addition, while ASL and DSC-MRI offer good sensitivity to perfusion

changes during stroke recovery, alterations in CBF and CBV may reflect vasodilation or metabolic changes (Figure 2), so these perfusion measures may not offer a high specificity for angiogenesis per se. Similarly, an increase in  $K_i$  (from DCE-MRI) or a shortening of  $T_2^*$  may arise because of other vascular pathology.<sup>25</sup> SSCE-MRI measures of microvascular density and vessel size arguably offer the greatest specificity for angiogenesis, but currently suffer from limited availability, especially within the clinical setting.

### ***Neurogenesis***

There are inherent limitations of resolution and sensitivity that preclude the direct visualization of endogenous neurogenesis. The unique metabolic properties of newly generated cells, however, can serve as surrogate markers. Magnetic resonance spectroscopy (MRS) potentially allows the *in vivo* measurement of marker compounds associated with different cell types. The metabolites most frequently detected in the human brain include choline, creatine, glutamate, glutamine, lactate, myo-inositol (mI), and N-acetyl aspartate (NAA), but there are at least 25 other less common metabolites that can be assessed by MRS.<sup>40</sup> Proton ( $^1\text{H}$ ) MRS offers better sensitivity compared to other nuclei (phosphorus or carbon) and is more likely to detect minor changes in metabolites.<sup>40</sup>

*In vitro* nuclear magnetic resonance (NMR) spectroscopy, a correlate of *in vivo* MRS, can identify cultured neurons, glial and meningeal cells by their metabolic properties.<sup>41</sup> Cultured neural stem cells exhibit high levels of choline and mI, and low concentrations of creatine, a profile different from embryonic stem cells or mature cells of the central nervous system.<sup>42</sup> A spectroscopic peak at 1.28 parts per million (ppm), found in cultured cells and the rat and human hippocampi, has been reported as being unique to neural progenitor cells, although this specificity has subsequently been questioned.<sup>43-47</sup>



A variety of metabolites in the peri-lesion area can inform on cellular repair mechanisms. Both single- and multiple-voxel MRS techniques have been used to non-invasively measure *in vivo* alterations of metabolite profile during stroke recovery in both human studies and in animal models.  $^1\text{H}/^{13}\text{C}$  MRS showed significant decrease in NAA, choline, and glutamate/glutamine turnover with increased glutamine and lactate at 24 hours in the perilesional areas of the rat brain, followed by normalization of NAA, choline, glutamine, and glutamate/glutamine turnover at 3 weeks, paralleling neurological improvement.<sup>48</sup> These alterations in the metabolite profile indicate substantial recovery of the initially impaired neural and glial functioning in the lesion border zone over time.<sup>48</sup> In humans, acute stroke is associated with elevated lactate and reduced NAA in the infarct zone, whereas the peri-infarct regions are characterised by lactate levels similar to the core but with NAA concentrations significantly higher than inside the infarct.<sup>49, 50</sup> In a longitudinal multi-voxel MRS study of 51 stroke patients, NAA concentrations fell both in infarcted and ipsilesional normal tissue over the first 2 weeks, and remained lower than baseline at 3 months, indicating neuronal loss.<sup>51</sup> A biphasic lactate peak was thought to represent initial tissue hypoxia followed by infiltration by inflammatory cells with a high rate of anaerobic glycolysis.<sup>51</sup> In another study, higher ml concentrations in the spared ipsi- and contra-lesional primary motor cortices of chronic stroke patients were thought to reflect astrocyte mediated post-stroke plasticity rather than gliosis.<sup>52</sup>

MRI contrast labelling offers an alternative approach for *in vivo* imaging of cellular elements during recovery.<sup>5, 53, 54</sup> Animal studies have employed superparamagnetic (iron oxide-based) particles and paramagnetic (gadolinium or manganese-based) agents, some of which are approved for human use.<sup>5</sup> Paramagnetic agents generate a hyperintense signal on  $T_1$ -weighted MRI, whereas cells harbouring even a single micron-sized iron oxide particle can be seen as

hypointense spots on T<sub>2</sub> and T<sub>2</sub>\*-weighted MRI, enabling precise anatomical localization and tracking of cell migration.<sup>55</sup> Neural stem cells labelled *in vitro* have successfully been detected *in vivo* in animal stroke models by means of MRI following transplantation (Figure 1).<sup>5, 56, 57</sup> A patient receiving an intravenous injection of iron-oxide microbead-labeled bone marrow stem cells 2 weeks after an ischemic stroke developed hypointensity compatible with iron (stem cell) deposition in the infarct, as detected with T<sub>2</sub>\* MRI 4 days after the injection.<sup>58</sup> Animal studies also indicate that endogenous neuronal stem/progenitor cells can also be labelled using cerebroventricular injections of MRI contrast agents, but their application in humans may be limited.<sup>55</sup> Labelling can alter cellular functional characteristics, and may not allow reliable differentiation between viable and dead cells; and uptake of contrast by other cell types such as phagocytes cannot be excluded.<sup>5, 53, 57, 59</sup>

MRI approaches to detect cellular changes during stroke recovery include the identification of progenitor cells by their unique metabolic profile or by labeling with contrast agents. (<sup>1</sup>H) MRS is available as an option on many commercial (human) MRI scanners, although more interactive optimisation is often required than is usual for MRI scanning, and considerable local expertise is necessary to ensure high quality data. MRS has low sensitivity, which is a major limitation if there are very few cells to detect, as is the case in the peri-lesion area harbouring sparsely seeded neural progenitors. The low sensitivity also means that large imaging voxels are required, which leads to partial volume effects and makes longitudinal follow-up harder as the relative concentrations of different components within a voxel may change over time. Furthermore, there is no one to one mapping of metabolites to cell types, which affects specificity.

***Axonal remodeling and cortical changes***

Diffusion tensor imaging (DTI) delineates anatomical connectivity of white matter pathways and can detect tract disruption.<sup>60</sup> DTI provides two scalar measures, the apparent diffusion coefficient (ADC) and fractional anisotropy (FA), which characterize the magnitude of water diffusion and the degree of anisotropy for each voxel (Figure 3).<sup>24</sup> In addition, careful interpretation of axial (parallel to the long axis of the fiber) and radial (perpendicular) diffusivity provides measures of axonal and myelination status, respectively.<sup>24, 61</sup>

Experimental stroke in rats has been characterized by decreased FA in perilesional areas at 3 days, followed by return to control values after 9 weeks.<sup>62</sup> In rat models of stroke, treatment with neural progenitor cells, sildenafil or erythropoietin has been associated with increased elevation of FA in peri-infarct areas at 5-7 weeks, which has correlated with reorganization of axons and myelin on histology, and with improved functional outcome.<sup>30, 63, 64</sup> In humans, a decrease in FA of the ipsilesional corticospinal tract has been detected during the first 3 months following ischemic stroke.<sup>65</sup> Early fiber tract degeneration has paralleled impaired recovery,<sup>66</sup> and predicted long-term deficits.<sup>65</sup> During a period of up to a few years after stroke, human studies (including some using specific interventions such as intonation-based speech therapy or brain-computer interface training)<sup>67, 68</sup> have observed increasing FA, connectivity and fiber number in lesioned and non-lesioned white matter, correlating with better functional outcome.<sup>67-71</sup> DTI evaluation of motor tract integrity in chronic stroke patients can predict motor function and behavioural gains from robotic therapy, motor practice, transcranial direct current or epidural motor cortex stimulation.<sup>72-77</sup>

DTI methods incorporating a single tensor fit to the diffusion at each voxel show an anomalous overall lowering of FA where white matter fiber tracts cross, despite the presence

of highly oriented tissue.<sup>24</sup> Newer q-space based and High Angular Resolution Diffusion Imaging (HARDI) techniques (e.g. diffusion spectrum imaging (DSI), q-ball, and persistent angular structure MRI (PAS-MRI)) provide model-independent analysis to obtain multiple tensors per voxel and thereby extract information on complex tissue structure including crossing fiber tracts.<sup>60, 78-80</sup> These techniques are particularly relevant in detecting randomly oriented crossing axons during early-stage axonal remodeling in stroke recovery.<sup>60</sup> In addition, changes in axonal density associated with stroke recovery can be measured using MRI diffusion entropy, a technique not dependent on axonal orientation.<sup>60</sup>

Manganese-enhanced MRI (MEMRI) is a novel tool for *in vivo* assessment of neuronal networks.<sup>81</sup> MEMRI is based on the detection of manganese ( $Mn^{2+}$ ), which enters active neurons and is transported axonally and trans-synaptically.<sup>81</sup> Paramagnetic manganese shortens the  $T_1$  relaxation time and increases signal intensity on  $T_1$ -weighted MRI. In a rat stroke model, decreased manganese enhancement in the ipsilateral sensorimotor network at 2 weeks after stroke was followed by enhanced connectivity on MEMRI and histology at 10 weeks, which correlated with behavioural recovery.<sup>82</sup>

MRI also allows the measurement of cortical thickness and gray matter density or volume.<sup>83,</sup>  
<sup>84</sup> In chronic stroke patients, atrophy of gray matter in remote brain regions (likely a consequence of impaired connectivity) predicted a lesser extent of motor improvement from subsequent constraint-induced movement therapy or epidural motor cortex stimulation.<sup>72, 85</sup> Increases in gray matter have been demonstrated in compensatory brain regions of chronic stroke patients,<sup>86</sup> and following constraint-induced movement therapy in parallel with functional improvements.<sup>87</sup> The mechanism of this increase in gray matter is likely to be multifactorial involving both neural and non-neural elements.<sup>86</sup>

In summary, DTI and MEMRI are potent *in vivo* techniques to study white matter structure, and MRI also provides tools to measure dimensions of gray matter. DTI is available either as standard or as an option on most commercial MRI scanners, which also routinely provide volumetric T1-weighted measurements. However there are potential limitations. The interpretation of tractography data requires experience and knowledge of white matter anatomy. Complex analytic methods are computationally demanding, and require longer processing times.<sup>88</sup> Several tractography algorithms have been described, but there is no consensus on the best method to use. Only few studies have validated tractography with dissection or histology, and knowledge on the relationship of MR measures and specific axonal events is limited. DTI cannot differentiate anterograde from retrograde connections or determine whether a pathway is functional.<sup>88</sup> Manganese is neurotoxic at high concentrations or after chronic exposure, which limits MEMRI-based neuronal tracing in human studies.<sup>89</sup>

### **General considerations for human application and future directions**

Non-invasive MRI biomarkers may provide deeper insights into specific neural events underlying stroke recovery. Furthermore, they may prove helpful to estimate prognosis, and identify patients who may benefit from specific interventions.<sup>90, 91</sup> The use of MRI biomarkers as surrogate end points may facilitate the screening of novel therapeutic interventions prior to large clinical trials. Considerations for surrogate markers should include feasibility of translation from animal to human studies, causal role in the disease process, and capacity to capture the net effect of therapy on clinical outcome.<sup>91</sup> MRI may not be the best brain-mapping tool for every aspect of stroke recovery: PET has a higher potential to characterize regional brain metabolism, and receptor and transporter distribution and

density;<sup>6</sup> transcranial magnetic stimulation (TMS) has advantages in evaluating the physiological properties of neural populations;<sup>92</sup> whereas magnetoencephalography (MEG) offers superior temporal resolution.<sup>93</sup>

The use of MRI to monitor recovery in humans presents additional challenges. There are well-known contraindications to MRI, and the administration of contrast agents may cause complications, particularly if given on multiple occasions.<sup>94, 95</sup> The most feasible clinical research protocols for the study of large patient populations in a longitudinal fashion would employ non-contrast techniques that are available on current scanner platforms (Table 1), with keeping in mind that sessions longer than 60 minutes are unlikely to be easily tolerated by most stroke patients. Imaging biomarkers are time dependent: some may be most useful to monitor recovery early after stroke (e.g. CBF),<sup>25</sup> whereas others may have limited value in the very early phase (e.g. FA may be transiently elevated on DTI as a consequence of edema).<sup>96</sup> The selection of regions of interest (ROI) for quantitative MRS, perfusion, or diffusion measurements requires hypotheses about the areas likely to be involved in post-stroke recovery, and focal abnormalities are often much easier to interpret if data from presumed normal tissue in the contralesional hemisphere are available for comparison.<sup>40</sup> It is also advisable that studies for research purposes use age-, gender-, and anatomically matched data from control subjects for comparison.<sup>40</sup>

Developments in MRI technology such as higher field strengths and faster MR acquisition methods will shorten scan times and make complex measurements more feasible. Further advantages of high field include improved spectral resolution, allowing the detection of more compounds with MRS,<sup>40</sup> and direct visualization of brain structures such as specific major fibre bundles.<sup>97</sup> However, high-field MRI is also associated with more prominent artefacts.<sup>98</sup>

Molecular imaging is another promising approach which may in future become more readily available. This may allow the monitoring of angiogenesis using paramagnetic contrast agents targeted against endothelial integrin  $\alpha_v\beta_3$ .<sup>99, 100</sup> Molecular MRI techniques for tracking cellular elements include imaging reporter genes (either with or without exogenous contrast administration) or contrast agent linked to receptor-specific antibodies.<sup>5, 53</sup> Contrast materials based on a heteronuclear (e.g.  $^{19}\text{F}$  or  $^{13}\text{C}$ ) approach, or 'responsive' agents that change contrast due to their altered magnetic properties (e.g. relaxation or chemical shift) in response to dynamic changes in physiological, enzymatic and other metabolic properties are other potential advances.<sup>53</sup>

### **Sources of funding**

This work was supported by a research grant from The Stroke Association, UK (TSA 2009/04).

### **Disclosure**

Dr. Sztriha receives research support from The Stroke Association, UK.

Dr. O'Gorman receives research support from The Stroke Association, UK.

Dr. Modo receives research support from the EU Framework VII (201842-ENCITE).

Dr. Barker receives research support from The Stroke Association, UK, and has received honoraria from General Electric.

Dr. Williams reports no disclosures.

Dr. Kalra receives research support from The Stroke Association, UK.

## References

1. Langhorne P, Bernhardt J, Kwakkel G. Stroke rehabilitation. *Lancet* 2011;377:1693-702.
2. Zhang ZG, Chopp M. Neurorestorative therapies for stroke: underlying mechanisms and translation to the clinic. *Lancet Neurol* 2009;8:491-500.
3. Hachinski V, Donnan GA, Gorelick PB, Hacke W, Cramer SC, Kaste M, et al. Stroke: working toward a prioritized world agenda. *Stroke* 2010;41:1084-99.
4. Dimyan MA, Cohen LG. Neuroplasticity in the context of motor rehabilitation after stroke. *Nat Rev Neurol*. 2011;7:76-85.
5. Gera A, Steinberg GK, Guzman R. In vivo neural stem cell imaging: current modalities and future directions. *Regen Med* 2010;5:73-86.
6. Eliassen JC, Boespflug EL, Lamy M, Allendorfer J, Chu WJ, Szaflarski JP. Brain-mapping techniques for evaluating poststroke recovery and rehabilitation: a review. *Top Stroke Rehabil*. 2008;15:427-50.
7. Rueger MA, Backes H, Walberer M, Neumaier B, Ullrich R, Simard ML, et al. Noninvasive imaging of endogenous neural stem cell mobilization in vivo using positron emission tomography. *J Neurosci*. 2010;30:6454-60.
8. Zhang ZG, Zhang L, Tsang W, Soltanian-Zadeh H, Morris D, Zhang R, et al. Correlation of VEGF and angiopoietin expression with disruption of blood-brain barrier and angiogenesis after focal cerebral ischemia. *J Cereb Blood Flow Metab* 2002;22:379-92.
9. Krupinski J, Kaluza J, Kumar P, Kumar S, Wang JM. Role of angiogenesis in patients with cerebral ischemic stroke. *Stroke* 1994;25:1794-8.
10. Zhang ZG, Zhang L, Jiang Q, Zhang R, Davies K, Powers C, et al. VEGF enhances angiogenesis and promotes blood-brain barrier leakage in the ischemic brain. *J Clin Invest* 2000;106:829-38.
11. Arvidsson A, Collin T, Kirik D, Kokaia Z, Lindvall O. Neuronal replacement from endogenous precursors in the adult brain after stroke. *Nat Med* 2002;8:963-70.
12. Parent JM, Vexler ZS, Gong C, Derugin N, Ferriero DM. Rat forebrain neurogenesis and striatal neuron replacement after focal stroke. *Ann Neurol* 2002;52:802-13.
13. Zhang RL, Chopp M, Gregg SR, Toh Y, Roberts C, Letourneau Y, et al. Patterns and dynamics of subventricular zone neuroblast migration in the ischemic striatum of the adult mouse. *J Cereb Blood Flow Metab* 2009;29:1240-50.
14. Thored P, Wood J, Arvidsson A, Cammenga J, Kokaia Z, Lindvall O. Long-term neuroblast migration along blood vessels in an area with transient angiogenesis and increased vascularization after stroke. *Stroke* 2007;38:3032-9.



15. Ohab JJ, Fleming S, Blesch A, Carmichael ST. A neurovascular niche for neurogenesis after stroke. *J Neurosci* 2006;26:13007-16.
16. Minger SL, Ekonomou A, Carta EM, Chinoy A, Perry RH, Ballard CG. Endogenous neurogenesis in the human brain following cerebral infarction. *Regen Med* 2007;2:69-74.
17. Macas J, Nern C, Plate KH, Momma S. Increased generation of neuronal progenitors after ischemic injury in the aged adult human forebrain. *J Neurosci* 2006;26:13114-9.
18. Martí-Fàbregas J, Romaguera-Ros M, Gómez-Pinedo U, Martínez-Ramírez S, Jiménez-Xarrié E, Marín R, et al. Proliferation in the human ipsilateral subventricular zone after ischemic stroke. *Neurology* 2010;74:357-65.
19. Jin K, Wang X, Xie L, Mao XO, Zhu W, Wang Y, et al. Evidence for stroke-induced neurogenesis in the human brain. *Proc Natl Acad Sci U S A* 2006;103:13198-202.
20. Li S, Overman JJ, Katsman D, Kozlov SV, Donnelly CJ, Twiss JL, et al. An age-related sprouting transcriptome provides molecular control of axonal sprouting after stroke. *Nat Neurosci* 2010;13:1496-504.
21. Benowitz LI, Carmichael ST. Promoting axonal rewiring to improve outcome after stroke. *Neurobiol Dis* 2010;37:259-66.
22. Dancause N, Barbay S, Frost SB, Plautz EJ, Chen D, Zoubina EV, et al. Extensive cortical rewiring after brain injury. *J Neurosci* 2005;25:10167-79.
23. Liu Z, Li Y, Zhang ZG, Cui X, Cui Y, Lu M, et al. Bone marrow stromal cells enhance inter- and intracortical axonal connections after ischemic stroke in adult rats. *J Cereb Blood Flow Metab* 2010;30:1288-95.
24. Jiang Q, Zhang ZG, Chopp M. MRI of stroke recovery. *Stroke* 2010;41:410-4.
25. Seevinck PR, Deddens LH, Dijkhuizen RM. Magnetic resonance imaging of brain angiogenesis after stroke. *Angiogenesis* 2010;13:101-11.
26. Rosen BR, Belliveau JW, Vevea JM, Brady TJ. Perfusion imaging with NMR contrast agents. *Magn Reson Med* 1990;14:249-65.
27. Jiang Q, Zhang ZG, Ding GL, Zhang L, Ewing JR, Wang L, et al. Investigation of neural progenitor cell induced angiogenesis after embolic stroke in rat using MRI. *Neuroimage* 2005;28:698-707.
28. Lin TN, Sun SW, Cheung WM, Li F, Chang C. Dynamic changes in cerebral blood flow and angiogenesis after transient focal cerebral ischemia in rats. Evaluation with serial magnetic resonance imaging. *Stroke* 2002;33:2985-91.
29. Williams DS, Detre JA, Leigh JS, Koretsky AP. Magnetic resonance imaging of perfusion using spin inversion of arterial water. *Proc Natl Acad Sci U S A* 1992;89:212-6.

30. Ding G, Jiang Q, Li L, Zhang L, Zhang ZG, Ledbetter KA, et al. Magnetic resonance imaging investigation of axonal remodeling and angiogenesis after embolic stroke in sildenafil-treated rats. *J Cereb Blood Flow Metab* 2008;28:1440-8.
31. Wu EX, Tang H, Jensen JH. High-resolution MR imaging of mouse brain microvasculature using the relaxation rate shift index Q. *NMR Biomed* 2004;17:507-12.
32. Jensen JH, Chandra R. MR imaging of microvasculature. *Magn Reson Med* 2000;44:224-30.
33. Lin CY, Chang C, Cheung WM, Lin MH, Chen JJ, Hsu CY, et al. Dynamic changes in vascular permeability, cerebral blood volume, vascular density, and size after transient focal cerebral ischemia in rats: evaluation with contrast-enhanced magnetic resonance imaging. *J Cereb Blood Flow Metab* 2008;28:1491-501.
34. Tofts PS, Kermode AG. Measurement of the blood-brain barrier permeability and leakage space using dynamic MR imaging. 1. Fundamental concepts. *Magn Reson Med* 1991;17:357-67.
35. Tofts PS, Brix G, Buckley DL, Evelhoch JL, Henderson E, Knopp MV, et al. Estimating kinetic parameters from dynamic contrast-enhanced T(1)-weighted MRI of a diffusable tracer: standardized quantities and symbols. *J Magn Reson Imaging* 1999;10:223-32.
36. Ding G, Jiang Q, Li L, Zhang L, Zhang ZG, Ledbetter KA, et al. Angiogenesis detected after embolic stroke in rat brain using magnetic resonance T2\*WI. *Stroke* 2008;39:1563-8.
37. Ogawa S, Lee TM, Kay AR, Tank DW. Brain magnetic resonance imaging with contrast dependent on blood oxygenation. *Proc Natl Acad Sci U S A* 1990;87:9868-72.
38. Sehgal V, Delproposto Z, Haacke EM, Tong KA, Wycliffe N, Kido DK, et al. Clinical applications of neuroimaging with susceptibility-weighted imaging. *J Magn Reson Imaging* 2005;22:439-50.
39. Calamante F, Thomas DL, Pell GS, Wiersma J, Turner R. Measuring cerebral blood flow using magnetic resonance imaging techniques. *J Cereb Blood Flow Metab*. 1999;19:701-35.
40. Barker PB, Lin DDM. In vivo proton MR spectroscopy of the human brain. *Progress in Nuclear Magnetic Resonance Spectroscopy* 2006;49:99-128.
41. Urenjak J, Williams SR, Gadian DG, Noble M. Proton nuclear magnetic resonance spectroscopy unambiguously identifies different neural cell types. *J Neurosci* 1993;13:981-9.
42. Jansen JF, Shambloott MJ, van Zijl PC, Lehtimäki KK, Bulte JW, Gearhart JD, et al. Stem cell profiling by nuclear magnetic resonance spectroscopy. *Magn Reson Med* 2006;56:666-70.
43. Manganas LN, Zhang X, Li Y, Hazel RD, Smith SD, Wagshul ME, et al. Magnetic resonance spectroscopy identifies neural progenitor cells in the live human brain. *Science* 2007;318:980-5.

44. Hoch JC, Maciejewski MW, Gryk MR. Comment on "magnetic resonance spectroscopy identifies neural progenitor cells in the live human brain". *Science* 2008;321:640.
45. Friedman SD. Comment on "Magnetic resonance spectroscopy identifies neural progenitor cells in the live human brain". *Science* 2008;321:640.
46. Jansen JF, Gearhart JD, Bulte JW. Comment on "Magnetic resonance spectroscopy identifies neural progenitor cells in the live human brain". *Science* 2008;321:640.
47. Ramm P, Couillard-Despres S, Plötz S, Rivera FJ, Krampert M, Lehner B, et al. A nuclear magnetic resonance biomarker for neural progenitor cells: is it all neurogenesis? *Stem Cells* 2009;27:420-3.
48. van der Zijden JP, van Eijssden P, de Graaf RA, Dijkhuizen RM. <sup>1</sup>H/<sup>13</sup>C MR spectroscopic imaging of regionally specific metabolic alterations after experimental stroke. *Brain* 2008;131:2209-19.
49. Gillard JH, Barker PB, van Zijl PC, Bryan RN, Oppenheimer SM. Proton MR spectroscopy in acute middle cerebral artery stroke. *AJNR Am J Neuroradiol* 1996;17:873-86.
50. Cvorovic V, Marshall I, Armitage PA, Bastin ME, Carpenter T, Rivers CS, et al. MR diffusion and perfusion parameters: relationship to metabolites in acute ischaemic stroke. *J Neurol Neurosurg Psychiatry* 2010;81:185-91.
51. Muñoz Maniega S, Cvorovic V, Chappell FM, Armitage PA, Marshall I, Bastin ME, et al. Changes in NAA and lactate following ischemic stroke: a serial MR spectroscopic imaging study. *Neurology* 2008;71:1993-9.
52. Cirstea CM, Brooks WM, Craciunas SC, Popescu EA, Choi IY, Lee P, et al. Primary motor cortex in stroke: a functional MRI-guided proton MR spectroscopic study. *Stroke* 2011;42:1004-9.
53. Himmelreich U, Dresselaers T. Cell labeling and tracking for experimental models using magnetic resonance imaging. *Methods* 2009;48:112-24.
54. Modo M, Mellor K, Cash D, Fraser SE, Meade TJ, Price J, et al. Mapping transplanted stem cell migration after a stroke: a serial, in vivo magnetic resonance imaging study. *Neuroimage* 2004;21:311-7.
55. Shapiro EM, Gonzalez-Perez O, Manuel García-Verdugo J, Alvarez-Buylla A, Koretsky AP. Magnetic resonance imaging of the migration of neuronal precursors generated in the adult rodent brain. *Neuroimage* 2006;32:1150-7.
56. Arbab AS, Janic B, Haller J, Pawelczyk E, Liu W, Frank JA. In Vivo Cellular Imaging for Translational Medical Research. *Curr Med Imaging Rev* 2009;5:19-38.
57. Modo M, Beech JS, Meade TJ, Williams SC, Price J. A chronic 1 year assessment of MRI contrast agent-labelled neural stem cell transplants in stroke. *Neuroimage* 2009;47:T133-42.

58. England TJ, Abaei M, Auer DP, Lowe J, Jones DR, Sare G, et al. Granulocyte-colony stimulating factor for mobilizing bone marrow stem cells in subacute stroke: the stem cell trial of recovery enhancement after stroke 2 randomized controlled trial. *Stroke*. 2012;43:405-11.
59. Vreys R, Vande Velde G, Krylychkina O, Vellema M, Verhoye M, Timmermans JP, et al. MRI visualization of endogenous neural progenitor cell migration along the RMS in the adult mouse brain: validation of various MPIO labeling strategies. *Neuroimage* 2010;49:2094-103.
60. Jiang Q, Zhang ZG, Chopp M. MRI evaluation of white matter recovery after brain injury. *Stroke* 2010;41:S112-3.
61. Wheeler-Kingshott CA, Cercignani M. About "axial" and "radial" diffusivities. *Magn Reson Med* 2009;61:1255-60.
62. van der Zijden JP, van der Toorn A, van der Marel K, Dijkhuizen RM. Longitudinal in vivo MRI of alterations in perilesional tissue after transient ischemic stroke in rats. *Exp Neurol* 2008;212:207-12.
63. Jiang Q, Zhang ZG, Ding GL, Silver B, Zhang L, Meng H, et al. MRI detects white matter reorganization after neural progenitor cell treatment of stroke. *Neuroimage* 2006;32:1080-9.
64. Li L, Jiang Q, Ding G, Zhang L, Zhang ZG, Li Q, et al. MRI identification of white matter reorganization enhanced by erythropoietin treatment in a rat model of focal ischemia. *Stroke* 2009;40:936-41.
65. Yu C, Zhu C, Zhang Y, Chen H, Qin W, Wang M, Li K. A longitudinal diffusion tensor imaging study on Wallerian degeneration of corticospinal tract after motor pathway stroke. *Neuroimage*. 2009;47:451-8.
66. Liang Z, Zeng J, Liu S, Ling X, Xu A, Yu J, Ling L. A prospective study of secondary degeneration following subcortical infarction using diffusion tensor imaging. *J Neurol Neurosurg Psychiatry*. 2007;78:581-6.
67. Schlaug G, Marchina S, Norton A. Evidence for plasticity in white-matter tracts of patients with chronic Broca's aphasia undergoing intense intonation-based speech therapy. *Ann N Y Acad Sci*. 2009;1169:385-94.
68. Caria A, Weber C, Brötz D, Ramos A, Ticini LF, Gharabaghi A, et al. Chronic stroke recovery after combined BCI training and physiotherapy: a case report. *Psychophysiology*. 2011;48:578-82.
69. Wang C, Stebbins GT, Nyenhuis DL, deToledo-Morrell L, Freels S, Gencheva E, et al. Longitudinal changes in white matter following ischemic stroke: a three-year follow-up study. *Neurobiol Aging* 2006;27:1827-33.

70. Pannek K, Chalk JB, Finnigan S, Rose SE. Dynamic corticospinal white matter connectivity changes during stroke recovery: a diffusion tensor probabilistic tractography study. *J Magn Reson Imaging* 2009;29:529-36.
71. Schaechter JD, Fricker ZP, Perdue KL, Helmer KG, Vangel MG, Greve DN, et al. Microstructural status of ipsilesional and contralesional corticospinal tract correlates with motor skill in chronic stroke patients. *Hum Brain Mapp* 2009;30:3461-74.
72. Nouri S, Cramer SC. Anatomy and physiology predict response to motor cortex stimulation after stroke. *Neurology*. 2011;77:1076-83.
73. Riley JD, Le V, Der-Yeghiaian L, See J, Newton JM, Ward NS, et al. Anatomy of stroke injury predicts gains from therapy. *Stroke*. 2011;42:421-6.
74. Stinear CM, Barber PA, Smale PR, Coxon JP, Fleming MK, Byblow WD. Functional potential in chronic stroke patients depends on corticospinal tract integrity. *Brain*. 2007;130:170-80.
75. Zhu LL, Lindenberg R, Alexander MP, Schlaug G. Lesion load of the corticospinal tract predicts motor impairment in chronic stroke. *Stroke*. 2010;41:910-5.
76. Lindenberg R, Renga V, Zhu LL, Betzler F, Alsop D, Schlaug G. Structural integrity of corticospinal motor fibers predicts motor impairment in chronic stroke. *Neurology*. 2010;74:280-7.
77. Lindenberg R, Zhu LL, Rüber T, Schlaug G. Predicting functional motor potential in chronic stroke patients using diffusion tensor imaging. *Hum Brain Mapp*. 2011 Apr 29. doi: 10.1002/hbm.21266.
78. Alexander DC, Barker GJ, Arridge SR. Detection and modeling of non-Gaussian apparent diffusion coefficient profiles in human brain data. *Magn Reson Med* 2002;48:331-40.
79. Hagmann P, Jonasson L, Maeder P, Thiran JP, Wedeen VJ, Meuli R. Understanding diffusion MR imaging techniques: from scalar diffusion-weighted imaging to diffusion tensor imaging and beyond. *Radiographics* 2006;26:S205-23.
80. Tuch DS, Reese TG, Wiegell MR, Wedeen VJ. Diffusion MRI of complex neural architecture. *Neuron* 2003;40:885-95.
81. Pautler RG. In vivo, trans-synaptic tract-tracing utilizing manganese-enhanced magnetic resonance imaging (MEMRI). *NMR Biomed* 2004;17:595-601.
82. van der Zijden JP, Bouts MJ, Wu O, Roeling TA, Bleys RL, van der Toorn A, et al. Manganese-enhanced MRI of brain plasticity in relation to functional recovery after experimental stroke. *J Cereb Blood Flow Metab*. 2008;28:832-40.
83. Fischl B, Dale AM. Measuring the thickness of the human cerebral cortex from magnetic resonance images. *Proc Natl Acad Sci U S A*. 2000;97:11050-5.

84. Ashburner J, Friston KJ. Voxel-based morphometry--the methods. *Neuroimage*. 2000;11:805-21.
85. Gauthier LV, Taub E, Mark VW, Barghi A, Uswatte G. Atrophy of spared gray matter tissue predicts poorer motor recovery and rehabilitation response in chronic stroke. *Stroke*. 2012;43:453-7.
86. Schaechter JD, Moore CI, Connell BD, Rosen BR, Dijkhuizen RM. Structural and functional plasticity in the somatosensory cortex of chronic stroke patients. *Brain*. 2006;129:2722-33.
87. Gauthier LV, Taub E, Perkins C, Ortmann M, Mark VW, Uswatte G. Remodeling the brain: plastic structural brain changes produced by different motor therapies after stroke. *Stroke*. 2008;39:1520-5.
88. Ciccarelli O, Catani M, Johansen-Berg H, Clark C, Thompson A. Diffusion-based tractography in neurological disorders: concepts, applications, and future developments. *Lancet Neurol*. 2008;7:715-27.
89. Silva AC, Lee JH, Aoki I, Koretsky AP. Manganese-enhanced magnetic resonance imaging (MEMRI): methodological and practical considerations. *NMR Biomed* 2004;17:532-43.
90. Milot MH, Cramer SC. Biomarkers of recovery after stroke. *Curr Opin Neurol* 2008;21:654-9.
91. Cramer SC, Sur M, Dobkin BH, O'Brien C, Sanger TD, Trojanowski JQ, et al. Harnessing neuroplasticity for clinical applications. *Brain*. 2011;134:1591-609.
92. Dimyan MA, Cohen LG. Contribution of transcranial magnetic stimulation to the understanding of functional recovery mechanisms after stroke. *Neurorehabil Neural Repair*. 2010;24:125-35.
93. Tecchio F, Zappasodi F, Tombini M, Oliviero A, Pasqualetti P, Vernieri F, et al. Brain plasticity in recovery from stroke: an MEG assessment. *Neuroimage*. 2006;32:1326-34.
94. Bellin MF. MR contrast agents, the old and the new (2006) *Eur J Radiol* 60:314-23.
95. Kanal E, Barkovich AJ, Bell C, Borgstede JP, Bradley WG Jr, Froelich JW, et al. ACR guidance document for safe MR practices: 2007. *Am J Roentgenol* 2007;188:1447-74.
96. Sotak CH. The role of diffusion tensor imaging in the evaluation of ischemic brain injury - a review. *NMR Biomed*. 2002;15:561-9.
97. Duyn J, Koretsky AP. Magnetic resonance imaging of neural circuits. *Nat Clin Pract Cardiovasc Med* 2008;5:S71-8.
98. Denic A, Macura SI, Mishra P, Gamez JD, Rodriguez M, Pirko I. MRI in rodent models of brain disorders. *Neurotherapeutics*. 2011;8:3-18.

99. Sipkins DA, Cheresh DA, Kazemi MR, Nevin LM, Bednarski MD, Li KC. Detection of tumor angiogenesis in vivo by alphaVbeta3-targeted magnetic resonance imaging. *Nat Med* 1998;4:623-6.
100. Winter PM, Morawski AM, Caruthers SD, Fuhrhop RW, Zhang H, Williams TA, et al. Molecular imaging of angiogenesis in early-stage atherosclerosis with alpha(v)beta3-integrin-targeted nanoparticles. *Circulation* 2003;108:2270-4.

## Figure legend

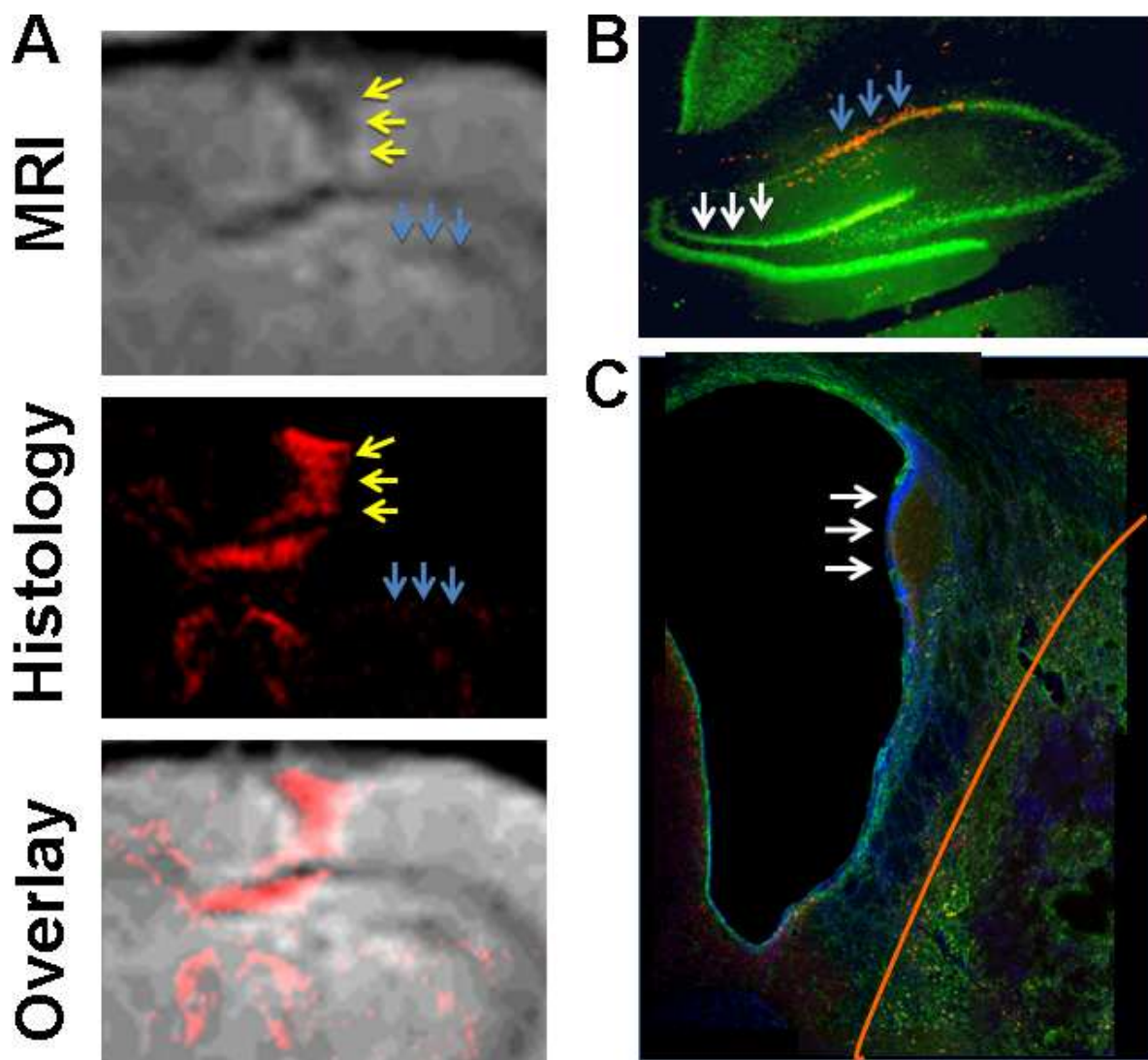


Figure 1. Imaging of transplanted and endogenous neural stem cells (NSCs)

A. Mouse neural stem cells labeled with a bimodal gadolinium-rhodamine (GRID) contrast agent can be detected both by MRI and fluorescence histology. The overlay of both images confirms good correspondence between the areas of transplanted cells on both imaging modalities. The blue arrows indicate the area of CA1 with transplanted cells, whereas the yellow arrows point to the injection tract.

B. In rats with global ischaemic damage (15 minutes of 4 vessel-occlusion), transplanted NSCs (in red due to rhodamine chelate from contrast agent) migrate into the CA1 cell layer



of the damaged hippocampus (NeuN<sup>+</sup> neurons marked in green), corresponding to the hippocampal region on the MR image (blue arrows). Detection of endogenous neurogenesis, however, constitutes a major challenge as only a small proportion of cells within the dentate gyrus (white arrows) are proliferating neural stem cells or newly generated neurons.

C. A similar challenge lies in the *in vivo* detection of neurogenesis in the sub-ependymal zone (SEZ, white arrows) next to the lateral ventricle. The SEZ is a very dense cellular region as can be seen here with DAPI (blue) labeling of every cell nucleus, delineating a thin line along the lateral ventricle. Although this zone is normally only a few cells deep, some parts of SEZ expand due to a stroke (area delineated with orange line), still remaining within approximately 100  $\mu\text{m}$  in thickness. *In vivo* ventricular motion as well as the dramatic variation in tissue type will be major challenges in the detection metabolic changes within this specific region. However, cells migrating into the peri-infarct area (astrocytes stained with GFAP are visible here in green) potentially can affect the metabolite profile of this area, although again the numbers infiltrating this area are relatively small compared to the overall volume of the peri-infarct area. Neuronal cells (NeuN in red) are dramatically decreased even in the peri-infract area, and very little cell replacement occurs due to endogenous neurogenesis.

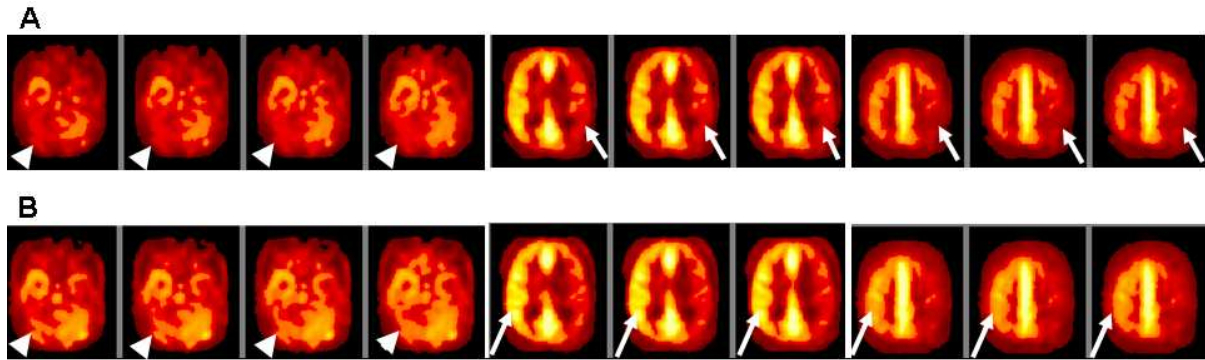


Figure 2. Group-average CBF maps using ASL in 6 patients with a cortical ischaemic stroke in the left middle cerebral artery territory. At 3 weeks after stroke (A) hypoperfusion in the affected hemisphere (arrows) and crossed-cerebellar diaschisis (arrowheads) is demonstrated. At 15 weeks perfusion (B, displayed with the same threshold as in A) is restored in the contralesional cerebellum (arrowheads), and is increased in the contralesional hemisphere (arrows).

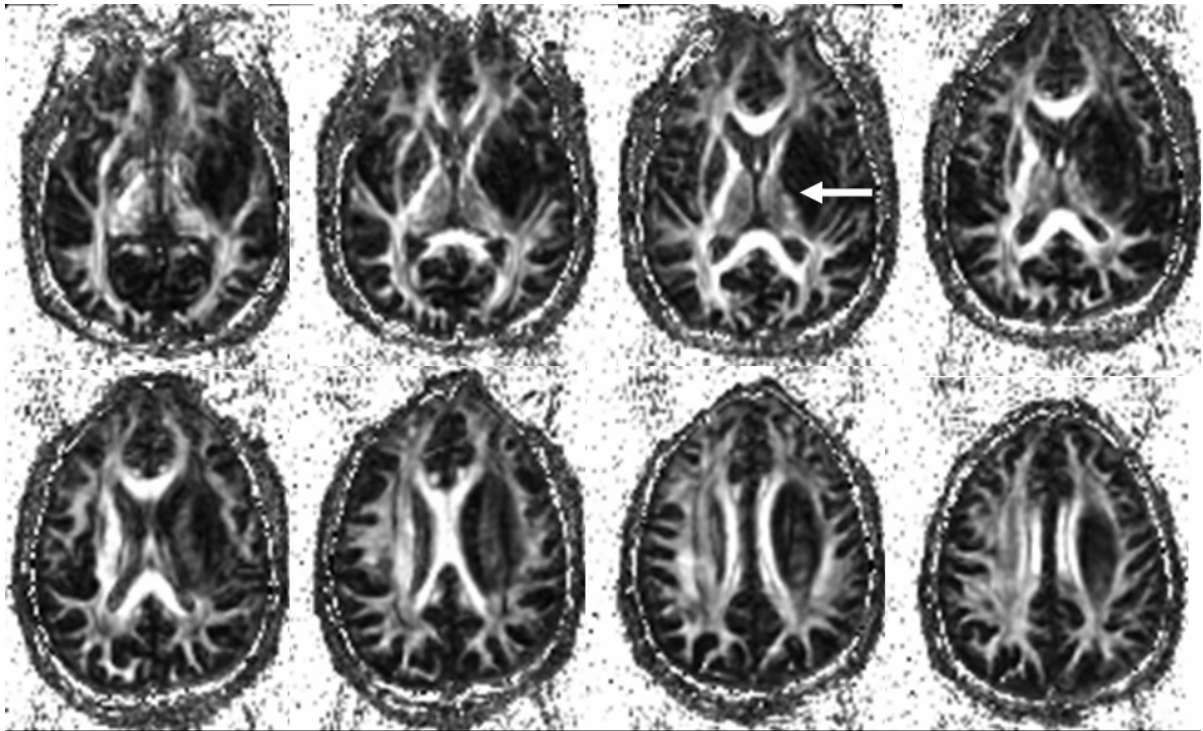


Figure 3. FA maps are easily obtainable on current scanners. FA values are decreased in the ipsilesional internal capsule (arrow) in a patient with left hemispheric ischaemic stroke.

Table 1. MR options for imaging post-stroke recovery

Technique	Need for exogenous contrast agent	Parameter measured	Availability on current scanner platform
<b>Angiogenesis</b>			
DSC-MRI	Yes	CBF, CBV	Yes
ASL	No	CBF	Yes
SSCE-MRI	Yes	Average vessel size, MVD	No
DCE-MRI	Yes	K <sub>i</sub>	No
Gradient/spin echo BOLD	No	Deoxygenated haemoglobin	Yes
SWI	No	Deoxygenated haemoglobin	Yes
<b>Cells</b>			
MRS	No	Concentrations of metabolites	Yes
Cell labeling	Yes	Properties of contrast in cells	No
<b>Axonal remodeling</b>			
DTI	No	ADC, FA, Q-space based and HARDI measurements	Yes
MEMRI	Yes	Paramagnetic manganese in neural networks	No
<b>Brain volume</b>			
T1-weighted volumetry	No	Regional gray matter volume	Yes

ADC, apparent diffusion coefficient; ASL, arterial spin labelling; BOLD, blood oxygenation level-dependent imaging; CBF, cerebral blood flow; CBV, cerebral blood volume; DCE-MRI, dynamic contrast-enhanced MRI; DSC-MRI, dynamic susceptibility contrast-enhanced MRI; DTI, diffusion tensor imaging; FA, fractional anisotropy; HARDI, High Angular Resolution Diffusion Imaging;  $K_i$ , blood brain barrier transfer constant; MEMRI, manganese-enhanced MRI; MRS, magnetic resonance spectroscopy; MVD, microvascular density; SSCE-MRI, steady state susceptibility contrast-enhanced MRI; SWI, susceptibility weighted imaging.